
Modeling the effects of the immune system and EMT on epithelial cancer progression

Daniel R. Bergman¹, Matthew K. Karikomi¹, Min Yu⁴, Qing Nie^{1,2,*}, and Adam L. MacLean^{1,3,*}

¹Department of Mathematics, University of California, Irvine, Irvine, CA 92697

²Department of Cell and Developmental Biology, University of California, Irvine, Irvine, CA 92697

³Department of Biological Sciences, University of Southern California, Los Angeles, CA 90089

⁴Department of Stem Cell & Regenerative Medicine, Keck School of Medicine, University of Southern California, Los Angeles, CA 90033

*Correspondence: qnie@uci.edu (Q.N.); macleana@usc.edu (A.L.M.).

During progression from carcinoma *in situ* to an invasive tumor, the immune system is engaged in complex sets of interactions with various tumor cells. Moreover, tumor cell plasticity can significantly alter disease trajectories via epithelial-to-mesenchymal transition (EMT). Several of the same pathways that regulate EMT are involved in tumor-immune interactions, yet little is known about the mechanisms and consequences of crosstalk between these regulatory processes. Here we introduce a multiscale evolutionary model to describe tumor-immune-EMT interactions and their impact on epithelial cancer progression from *in situ* to invasive disease. Through *in silico* analyses of large patient cohorts, we find controllable regimes that maximize invasion-free survival. We identify that delaying tumor progression depends crucially on properties of the mesenchymal tumor cell phenotype: its growth rate and its immune-evasiveness. Through analysis of inflammation-associated cancer data from The Cancer Genome Atlas, we find that – in agreement with model predictions – association with EMT significantly worsens invasion-free survival probabilities. These results offer novel means to delay disease progression by regulating properties of EMT, and demonstrate the importance of studying cancer-immune interactions in light of EMT.

¹ 1 Introduction

² The majority of deaths from cancer are due to metastasis of the disease [1]. It is thus of critical
³ importance to understand better the progression from *in situ* to invasive disease. Underlying
⁴ this progression are genetic and epigenetic events, including mutations in pathways critical to

5 the success of the cancer cell (driver mutations) [2]. These pathways include cell proliferation,
6 apoptosis, and immunogenicity.

7 Cancer and the immune system interact in myriad ways. The immune system modulates the
8 tumor microenvironment (TME), since immune signals that affect the tumor can be amplified
9 or repressed through feedback in response to local inflammatory signals. This complex cell
10 signaling occurs alongside the targeting (and potential eradication) of the tumor by immune
11 cells [3].

12 The effects of the immune system on a tumor can be broadly summarized into two branches.
13 The cytotoxic branch of the immune system, such as natural killer cells (NKs) and cytotoxic
14 T cells (CTLs), seek out and lyse tumor cells. Upon carrying out their effector functions,
15 these cytotoxic cells lose efficacy or deactivate [4]. The regulatory branch of the immune
16 system (Tregs, and other factors), inhibits the effective functioning of the cytotoxic branch [5].
17 Inflammation can increase the probability of cancer incidence and progression, with some of
18 the most pronounced effects seen for tumors originating in gastrointestinal and pancreatic
19 tissues [6, 7]. Recent work has shown, contrary to the typical effects of inflammation on cancer,
20 that under certain conditions inflammation may not be oncogenic but rather onco-protective [8].

21 Immunotherapies are beginning to realize their potential, with significant impacts on patient
22 health and survival [9, 10], and may even provide a cure for certain hematopoietic cancers
23 via anti-CD19 CAR-T cells [11]. The presentation of antigens on tumor cells is recognized by
24 innate immune cells that are transported to lymph nodes where T cells (and other components)
25 can be activated [12]. The tumor also engages in processes that can indirectly modify the TME,
26 for example by releasing transforming growth factor beta (TGF- β), which can shift the TME
27 towards a tumor-supportive environment by enhancing immunosuppression via activation of
28 Tregs [12].

29 Epithelial-to-mesenchymal transition (EMT) describes a reversible process by which cells dis-
30 playing an epithelial phenotype transition into cells with a mesenchymal phenotype. Epithelial
31 cells are – in part – defined by tight cell-cell adhesion. Mesenchymal cells exhibit less adhesion,
32 greater ranges of motility, and may possess stem-like properties [13], although controversy
33 regarding ‘stemness’ and EMT remains [14, 15]. Recent work has shown that – rather than
34 being a binary process – at least two stable intermediate EMT states exist [16, 17]. Ongoing
35 investigations into the plasticity and stability of EMT overlap with discussions elsewhere, e.g.
36 of discrete vs. continuous processes during cell differentiation [18]. Intermediate states have
37 emerged as a central mechanism by which cell fates (and the noise inherent within them) can
38 be controlled [19–21].

39 Two features of the mesenchymal phenotype are of particular relevance in the context
40 of cancer-immune interactions. i) mesenchymal tumor cells proliferate less than epithelial
41 cells, we refer to this as mesenchymal growth arrest (MGA), and can be considered related to
42 (in the sense of quiescence) the “stemness” phenotype of the mesenchymal tumor cells [22].
43 ii) mesenchymal cells are less susceptible to immune clearance [23]. As a cell is targeted
44 by cytotoxic immune cells for clearance, a physical connection between the two cells must
45 be established. This immunological synapse – mediated in part by T-cell receptors bound to
46 antigens and the major histocompatibility complex on the target cell – is down-regulated in
47 mesenchymal cells, thus inhibiting formation of the synapse [23]. We refer to this phenotype
48 as mesenchymal immune evasion (MIE).

49 In addition to the prominent role it plays in metastasis, EMT has more recently been shown

50 to also regulate other aspects of tumor progression [13, 24]. TGF- β , a master regulator of
51 EMT [25], is at once implicated heavily in tumor-mediated immune responses, since Tregs
52 release TGF- β upon arriving at the tumor site [23]. In hepatocellular carcinoma, for example,
53 there is direct evidence linking Treg-secreted TGF- β with EMT [26]. Thus, even by considering
54 only the TGF- β pathway, we find compelling evidence that these three core components (the
55 tumor, the immune system, and EMT) all interact. It therefore strikes us as a priority to develop
56 models to understand how the interactions between each of these three components affect
57 cancer incidence and progression.

58 Mathematical oncology, that is, mathematical models of cancer incidence, progression,
59 and treatment, has become a well-developed field; many models have offered insight into the
60 cellular interactions underlying cancer and its interplay with the immune system, including
61 older [27–29] and more recent works [30–43]. These studies have increased our understanding
62 of how tumors grow in the presence of various immune components, and how treatment regimes
63 can be designed to maximize the efficacy of cytotoxicity while minimizing risks to the patient.
64 However, to our knowledge no models have addressed how the effects of EMT alter interactions
65 between the immune system and cancer, and the subsequent implications for treatment.

66 Here we develop a model with the goal of studying interactions between the tumor, the
67 immune system and EMT. We seek to describe a set of crucial molecular and cellular interactions
68 in epithelial tumor cells, including effects due to DNA damage and mutation, to investigate
69 the probability that *in situ* tumors will progress and, if so, when. A recent model of cancer-
70 immune interactions [8] described the effects of the TME on the risk of cancer, and we build
71 on the core cell cycle component of this model, adding significant new interactions to the
72 immune component of the model (which was previously modeled by a single interaction), as
73 well as adding the effects of EMT. In doing so, we shift the focus of the previous model from
74 cancer initiation to cancer progression. We do this to reflect the fact that cancer progression
75 hinges on escape from the immune system and the fact that EMT has a more well-defined role
76 during progression and metastasis. We seek to understand whether this more complex immune
77 module will change our understanding of inflammatory effects on the tumor, and how the
78 epithelial-mesenchymal axis influences these.

79 In the next section we develop the model, explaining the intuition behind each of its
80 components. We go on to analyze its behavior: global “one-at-a-time” sensitivity analysis
81 identifies parameters that are crucial for progression. We study these in more depth, focusing
82 on the competing effects of EMT and of the immune system on progression, and discover
83 that EMT intricately regulates progression: under certain regimes a careful balance of EMT-
84 and immune-driven processes can significantly prolong invasion-free survival. To test these
85 predictions, we analyze data from the Cancer Genome Atlas (TCGA), and find evidence for the
86 synergistic effects of inflammation and EMT predicted by the model for patients with pancreatic
87 or ovarian cancer.

Quick Guide to Equations and Assumptions

To become invasive, An *in situ* tumor relies on mutations to alter cellular signaling pathways that enable cancer progression. The immune system simultaneously responds to the tumor upon recognition of neoantigens, and shapes the TME through dynamic inflammatory and regulatory signals.

To capture these dynamics, we developed a non-spatial agent-based model. Tumor cells are modeled individually as agents and immune cell populations are described homogeneously by differential equations. We consider two tumor cell types: epithelial tumor cells (ETCs) and mesenchymal tumor cells (MTCs). Time is treated discretely in 18 hour steps; approximately the time of one cell cycle. During each cell cycle, tumor cells can either undergo division, apoptosis, immune clearance, or can rest. The likelihood that a cell will proliferate depends on the tumor size (competition for resources) and on cell-intrinsic factors. The likelihood that a cell will undergo apoptosis is constant but varies between cell types (ETC and MTC). The likelihood of immune clearance depends on the number and type of mutated cells in the tumor, cytotoxicity, regulatory cells, and cell-intrinsic factors. As tumor cells proliferate, DNA damage can occur, and over time they become increasingly likely to acquire pathway mutations that change their propensities for proliferation or cell death. Natural killer (NK) cells identify and clear tumor cells, a process which results in neoantigens priming and activating T cells in local lymph nodes. T cells can subsequently infiltrate the TME. At the tumor site, cytotoxic T cells (CTLs) lyse tumor cells, and T regulatory cells (Tregs) suppress cytotoxic activity. The following equation determine the per-cell cycle probability that a tumor cell will be lysed by a CTL:

$$\rho_{\text{CTL}} = \delta_{\text{MUT}} \frac{N_{\text{CTL}}}{N_C/K_1 + N_{\text{CTL}}} \frac{E_{\text{CTL}}}{1 + N_{\text{Treg}}/K_2} (1 - \delta_{\text{IE}} \Delta_{\text{IE}}) (1 - \zeta \Delta_{\text{MIE}})$$

Here, δ_{MUT} is 1 or 0 depending on whether or not the cell has a mutation. The second term is a hill function modeled after [44] and the third term describes onco-protective effects of Tregs. The second-to-last term describes the increased immune-evasiveness that can occur following mutation in the immune evasion pathway, and the last term quantifies the additional immune evasiveness associated with MTCs. The inflammatory state of the TME thus impacts (through multiple factors) immune recruitment and cytotoxicity at the tumor site.

EMT impacts tumor cells through their proliferation and potential to evade the immune system change. MTCs have reduced proliferation and increased immune evasiveness TGF- β , an activator of EMT, is produced both by Tregs and tumor cells, thus connecting tumor-immune interactions with EMT, and as a result plays an important role in shaping tumor outcomes. To determine whether a cell undergoes EMT or MET, the TGF- β is randomly divided among the cells so that associated with each cell i is a value τ_i . This value is given by the following equation:

$$\tau_i = \frac{\tau_{\max}}{N_C} \frac{\tau/K_3}{1 + \tau/K_3} + X_i, \quad X_i \sim N(0, \sigma^2)$$

Here, τ is the concentration of TGF- β in the TME and τ_{\max} represents a limit on the amount

of TGF- β that can be absorbed by all cells, with Gaussian noise added. For each cell, τ_i is summed with the current EMT score for that cell and if the result is above a threshold value, the cell undergoes EMT, otherwise MET. This summation expresses the assumption that the epithelial and mesenchymal phenotypes are stable and cells will move along the EMT spectrum towards the equilibrium they identify as under typical conditions. Our goal is to determine when the cancer becomes invasive, determined through the proportion of tumor cells harboring mutations in pathways that permit escape from *in situ*, relative to the total tumor cell population.

88 **2 Methods**

89 Here we briefly describe to core components of the model. Full details and equations are
90 provided in the Supplement. We develop an agent-based model to describe the relationships
91 between cancer, the immune system, and EMT, building on the cell-cycle and tissue-cell compo-
92 nents described in [8]. The agents in the model are the cells that have already formed an *in*
93 *situ* tumor yet lack key pathway mutations to become invasive. In the process of the simulation,
94 these cells can acquire mutations altering any of three key pathways (Fig. 1A).

95 We model immune cells as continuous variables, i.e. we assume that the tumor microen-
96 vironment is well-mixed with regards to the infiltrating immune cells. The cytokine TGF- β is
97 also assumed to be well-mixed in the tumor microenvironment. Tumor cells can take on either
98 epithelial or mesenchymal phenotypes in a plastic manner: these phenotypes depend on both
99 the TME and cell-intrinsic factors. While the EMT score is continuous, a threshold determines
100 if a given cell is labeled as epithelial or mesenchymal (Fig. 1).

101 **2.1 Tumor evolution**

102 Associated with each tumor cells are two essential features: their mutational signature and their
103 EMT score. We consider three idealized pathways that can be mutated: proliferation, when
104 altered this increases the probability of the cell proliferating within each cell cycle; apoptosis,
105 when altered this decreases the probability of a cell undergoing apoptosis; and immune evasion,
106 when altered this decreases the probability that a mutated cell will be cleared by immune
107 components.

108 **2.2 Immune population dynamics**

109 The immune system is modeled by three immune cell types: NKs, CTLs, and Tregs. The NKs
110 and CTLs act on the system by recognizing invasive cells and clearing them. Upon clearance,
111 they are deactivated and removed from the immune population. Tregs suppress the function
112 of NKs and CTLs (reduce tumor cell clearance), and in addition, release TGF- β which further
113 shapes the TME by pushing tissues cells more towards a mesenchymal phenotype.

114 2.3 Periodic cycling inflammation states

115 Inflammation is modeled as a cycling scheme between low and high inflammatory states, with
116 varying on/off durations and intensities. For the purpose of simulation we consider the default
117 state to be low inflammation, and update the immune activity parameters whenever a switch
118 to the high state occurs. In the SI (Table S2) we give full details of parameter settings during
119 low and high inflammation.

120 2.4 Epithelial-to-mesenchymal transition

121 Each tissue cell has an EMT score between 0 and 1 with is set according to the concentration
122 of TGF- β in the TME. Above a threshold, the cell acquires the phenotype of a mesenchymal
123 tumor cell (MTC); otherwise, it is an epithelial tumor cell (ETC). For the purpose of simulation,
124 ETCs are considered to be in the base state, and MTCs will have a subset of their parameters
125 updated. In modeling EMT this way, we are assuming that the same factor, TGF- β , drives EMT
126 both at initiation and through progression of cancer.

127 Cells that have undergone EMT (i.e. MTCs) experience a reduction in proliferation, referred
128 to as mesenchymal growth arrest (MGA), and a decrease in the likelihood that they will be
129 cleared by immune cells (NKs or CTLs), referred to as mesenchymal immune evasion (MIE).
130 Both these parameters lie within the range [0, 1], thus we can sufficiently sample from their
131 joint parameter space to explore it in depth with the need for informative priors to constrain
132 their values.

133 2.5 Model simulation

134 **Initial conditions.** Simulations are initialized with N_0 in situ tumor cells, determined by the
135 choice of parameter values. A number of warmup cycles are run so that the model reaches
136 steady state. During warmup, no mutations occur, and the only immune cells present are NKs.
137 After warmup, mutations are permitted. Cells that do not mutate undergo an increase in their
138 probability of mutation in a later cell cycle.

139 **Tumor cell fate.** During each cell cycle, the fate of each cell is assigned: proliferation,
140 apoptosis, immune clearance, and rest in G_0 , according the model rules. The probability of
141 proliferation is affected by mutations to the proliferation pathway (increased) and my cells in a
142 mesenchymal state (decreased). Probabilities of immune clearance are affected by the number
143 of mutations harbored: cells with more mutations are assumed to be more immunogenic and
144 have a higher probability of being cleared by the immune system, unless the cell has a mutation
145 in the immune evasion pathway. Cells in a mesenchymal state can exhibit greater capacity to
146 evade immune clearance.

147 **Completing the cell cycle.** Once all tumor cells have been updated and fates chosen accord-
148 ingly, non-tumor model components are updated. Immune cell populations are updated in two
149 steps. First, immune cell exhaustion is calculated based on the number of tumor cells cleared,
150 e.g. clearance of one tumor cell by an NK cells results in the NK cell population decreasing
151 by one. Second, all immune cells (NKs, CTLs, Tregs) are updated according to a system of

152 coupled ordinary differential equations that govern their population dynamics. CTL and Treg
153 recruitment rates are dependent on the number of tumor cells; in addition TGF- β enhances the
154 recruitment rate of Tregs.

155 At the end of each cell cycle, new mutations can occur in cells that have undergone division,
156 according to cell-specific probabilities that increase if no mutation occurs are reset to 0 in the
157 event of a mutation. Finally, the concentration of TGF- β and the EMT score for each cell are
158 updated. Tregs and (to a lesser extent) invasive tumor cells are the sources of TGF- β ; the total
159 concentration per cell cycle is divided randomly among tumor cells. EMT is then assessed,
160 depending on the EMT score of the cell and the local concentration of TGF- β .

161 **Mutational burden and progression to invasive disease.** At the end of each cell cycle,
162 the proportion of tumor cells that are invasive is calculated based on their mutational burden,
163 and if it is above a certain threshold, the tumor is declared to have progressed to an invasive
164 state and the simulation ends. The time to invasion is calculated as the time from the start of
165 the simulation, minus the warmup period, until the invasive state is reached. Simulations run
166 until either this occurs or until the maximum number of cell cycles has been reached.

167 2.6 Parameter estimation and sensitivity analysis

168 To study parameter sensitivity, we implemented Morris a one-step-at-a-time global sensitivity
169 analysis. Parameters are varied one at a time from a set of sampled “base” points and the
170 resulting simulations recorded [45, 46]. For each run we simulated 1000 patients, and initialized
171 the Morris sampling with 30 points in parameter space (at least 10 are recommended in [46]).
172 Parameter sampling a choice of prior parameter distributions. For many parameters, such
173 as for the immune population dynamics, measurements or estimates were available from
174 literature [44]. For parameters such as MIE and MGA related to the mesenchymal phenotype,
175 little prior information was available, thus these was sampled across all possible values in [0, 1].
176 Tumor size in the model was scaled from cell numbers on the order of 10^9 cells [44] to the order
177 of 10^2 , and parameter values were scaled accordingly. Where parameter estimates existed, the
178 prior for parameter θ_i is given as $\theta_i \sim N(m_e, 2m_e)$, where m_e is the previous estimate and we
179 take twice this value as the variance to obtain a range of samples that does not rely too heavily
180 on previous work. The Morris algorithm computes the sensitivity, μ^* , as the average of the
181 absolute change of the output, which in our model is the area under the survival curve (Fig. 2).

182 2.7 Analysis of patient survival data from TCGA

183 We obtain primary tumor bulk mRNA sequencing and censored survival data for all individuals
184 monitored in the relevant project from the Cancer Genome Atlas (TCGA) from the Genomic
185 Data Commons portal in R, using the package TCGABiolinks. Given $n >= 1$ gene set keywords
186 (e.g. "inflammatory" and "emt"), the symbolic names of all msigdb gene sets are searched for
187 matches to these keywords, and matched gene sets are grouped by keyword. For each element
188 in the product S of all keyword groups, the following analysis is performed.

- 189 1. The first principle component of the expression across the gene set is obtained for each
190 element of the n-tuple of gene sets.

Name	Description
p	proliferation rate of tumor cells
d_C	death rate of tumor cells
Δ_{MIE}	mesenchymal immune evasion
Δ_{MGA}	mesenchymal growth arrest
Δ_A	decrease in apoptosis rate in cells with driver mutation in apoptosis pathway
Δ_{IE}	increase in immune evasion in cells with driver mutation in immune evasion pathway
Δ_P	increase in proliferation in cells with driver mutation in proliferation pathway
K_0	EC50 term for negative feedback of tumor cells on own proliferation
K_1	EC50 term for probability of NK cell finding mutant cell
K_2	EC50 term for Treg inhibition of cytotoxic functions
K_3	EC50 term for how much TGF- β each cell has
K_4	EC50 term for TGF- β activation of Tregs
E_{NK}	rate of NKs clearing mutants
E_{CTL}	rate of CTLs clearing mutants
σ_{NK}	NK source rate
σ_{CTL}	CTL source rate per cleared malignant cell
σ_{Treg}	Treg source rate per cleared malignant cell
d_{NK}	NK death rate
d_{CTL}	CTL death rate
d_{Treg}	Treg death rate
k_{EMT}	EMT/MET rate
σ	standard deviation of noise in TGF- β each cell receives
τ_{\max}	max amount of TGF- β any cell can receive
τ_{MUT}	rate of TGF- β production by mutant cells
τ_{Treg}	rate of TGF- β production by Treg

Table 1: Description of key model parameters. Note that some are not constant as they can be affected by the inflammation state of the system.

- 191 2. Two clusters of n-dimensional patient vectors are obtained by k-means clustering.
- 192 3. The patients are separated by their cluster identity and Kaplan-Meier curves are fit to
- 193 their corresponding survival data.
- 194 4. Under the null hypothesis that there is no difference between the survival of the two
- 195 groups, a log-rank test is performed.
- 196 5. The log-rank test p-value for each element in S is placed in an ordered list, the lowest of
- 197 which defines the element of S whose composite gene sets are most predictive of patient
- 198 survival in the given TCGA project or tumor type.

199 We apply this pipeline to several inflammation-associated cancers, denoted according to their
200 annotations in TCGA, including “PAAD” for pancreatic cancer, “OV” for ovarian cancer, and
201 “LIHC” for liver hepatocellular carcinoma.

202 3 Results

203 3.1 A multiscale agent-based model of EMT-immune-tumor cell interactions 204 to study tumor progression

205 We begin by investigating general features of the model to establish baseline conditions and
206 assess the impact of different model components on the key measured outcomes: the probability
207 of progression, and the time to invasion. Within the cell cycle, cell fate is determined by rules
208 that are influenced by EMT and immune interactions (Fig. 1A), e.g. if a cell undergoes EMT,
209 its probability of proliferation is reduced; if it gains a mutation in the apoptosis pathway, its
210 probability of apoptosis is reduced. Meanwhile, NK cells and CTLs attempt to clear malignant
211 tumor cells, and deactivate upon successful tumor cell clearance; Tregs inhibit this cytotoxic
212 activity (1A Inset).

213 The inflammation cycling scheme for a typical *in silico* patient consists of alternating high
214 and low regimes with corresponding effects on the cell populations (Fig. 1B). For this patient,
215 after warmup, mutations are observed at a rate low enough that they are cleared by cytotoxic
216 cells for about 700 cell cycles, after which the mutated and thus invasive cell population begins
217 to grow, leading to large recruitment of CTLs and Tregs and a peak in the concentration of
218 TGF- β . After 841 cell cycles, the proportion of invasive cells reaches 50%: the threshold defining
219 progression, thus this patient has a time to invasion of 841 cell cycles, or 631 days. Beyond this
220 timepoint, we see a rapid increase in the number of invasive cells until it comprises 100% of the
221 tumor population. Interesting EMT dynamics are also observed, the proportion of MTCs peaks
222 shortly after the tumor becomes invasive, subsequently the majority of cells transition back to an
223 epithelial state. We observe that while the NK population varies little over the simulation, CTLs
224 and Tregs both undergo large expansions. CTLs and Tregs also appear to oscillate, however
225 note that this is a direct result of the inflammation state, and is not immune cell-intrinsic.

226 In order to quantify patient dynamics and invasion-free survival as a population level, we
227 simulate large cohorts of patients similar to the single patient shown in Fig. 1B. For a cohort of
228 500 patients, we simulate survival curves and see that a large number progress quickly to form
229 invasive tumors, whereas a few lie in the tail of the distribution after the mutagenic event that
230 a large number of tumors quickly progress while others takes some time before progressing Fig.
231 1C. By approximately 1200 cell cycles (2.5 years), all tumors have become invasive..

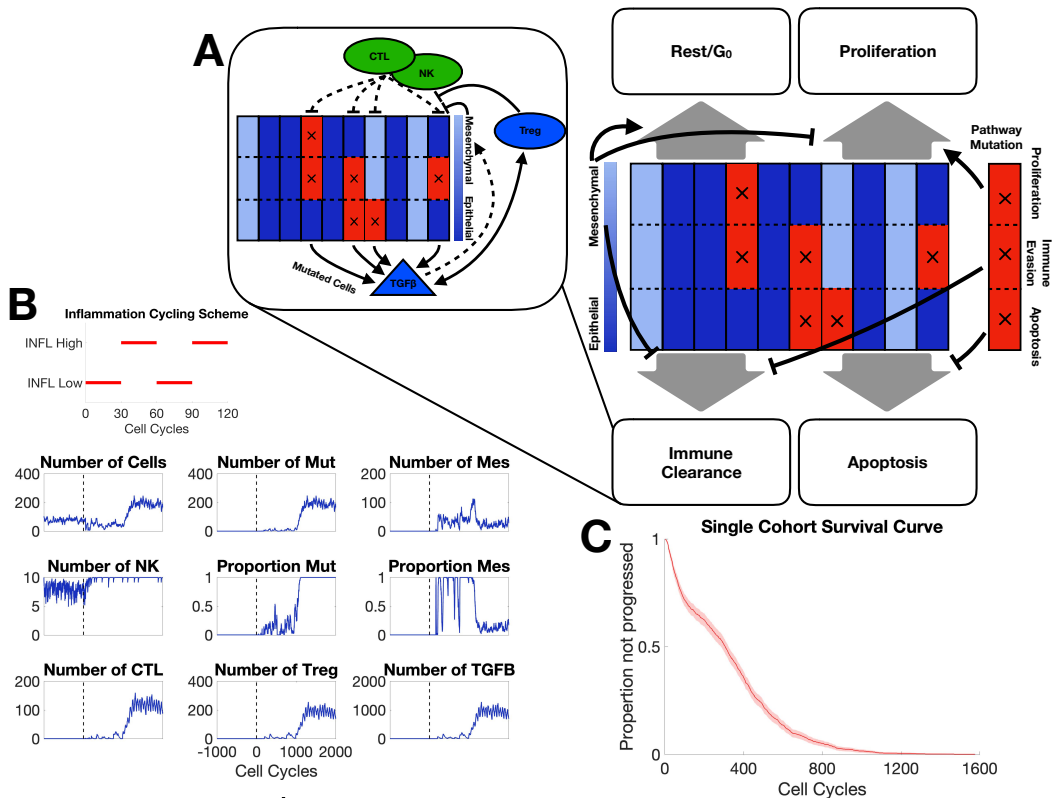


Figure 1: **A.** Schematic depiction of agent-based model components; each of the 10 columns represents a single tumor cell divided into three compartments representing the state (altered or not) of the three pathways with mutagenic potential; red/blue denotes altered/unaltered pathways. Black arrows depict regulation of the cell fate in each cell cycle. Inset depicts major interactions between the immune system and tumor cells. **B.** A representative simulation of one patient. The model parameter values used can be found in Table S2. The inflammation cycling scheme is represented above the patient dynamics. The vertical dashed line denotes the end of the warmup period. Mut: malignant cells; Mes: mesenchymal cells. **C.** Survival curve for one cohort of patients with the parameter values given in Table S2.

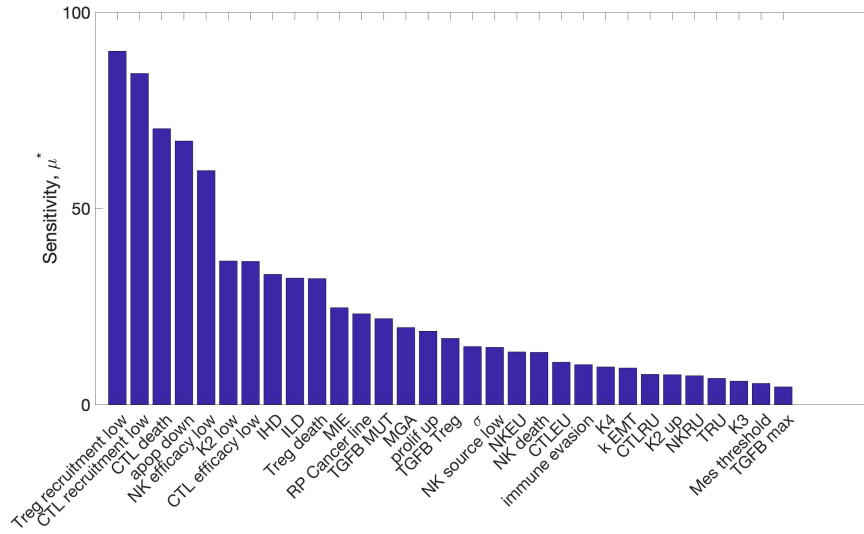


Figure 2: Global sensitivity analysis of model parameters. The sensitivity (μ^*) denotes the average absolute change in the time to invasion over the range of variation of the parameter.

232 3.2 Identification of key model parameters via global sensitivity analysis

233 Exploring the parameter spaces of systems biology models adequately is – in general – a
 234 hard problem. Fitting parameters via (Bayesian) parameter inference is advisable wherever
 235 possible [47]. Here, despite a wealth of data on tumor growth dynamics, a lack of sufficient
 236 molecular measurements (i.e. immune cell dynamics) precludes inference of the full model. In
 237 addition, while inference schemes for agent-based models are developing [48, 49], simulation
 238 times remain a hurdle [50]. Parameters for some components of the model studied previously
 239 can be constrained [8]. However, even here, new biological processes in the current system
 240 could push the model into new behavioral regimes. Thus to sample and characterize the
 241 parameter space of the model we use sensitivity analysis.

242 The results of Morris one-step-at-a-time sensitivity analysis on the 31 model parameters (Fig.
 243 2) find a subset of parameters with much higher levels of sensitivity than others. The two most
 244 influential by this analysis are the recruitment rates of Tregs and CTLs in the low inflammation
 245 state. The parameters influencing EMT are also identified as influencing model outcomes. Since
 246 one goal of our analysis is to assess the specific effects of EMT on immune-cancer dynamics,
 247 parameters MIE and MGA are of particular interest. In addition, inflammation parameters
 248 controlling the periodic high/low inflammation states are of interest because they strongly
 249 influence model outcomes and are capable of being targeted by therapeutic treatments. For
 250 immune cell dynamics, the secretion of TGF- β by Tregs is found to be sensitive and thus will
 251 also be studied further below.

252 3.3 Mesenchymal properties dramatically alter invasion-free survival times

253 Mesenchymal tumor cells (MTCs) are characterized by changes in two parameters: mesenchymal
 254 immune evasion (MIE) and mesenchymal growth arrest (MGA). Here we assess the effects

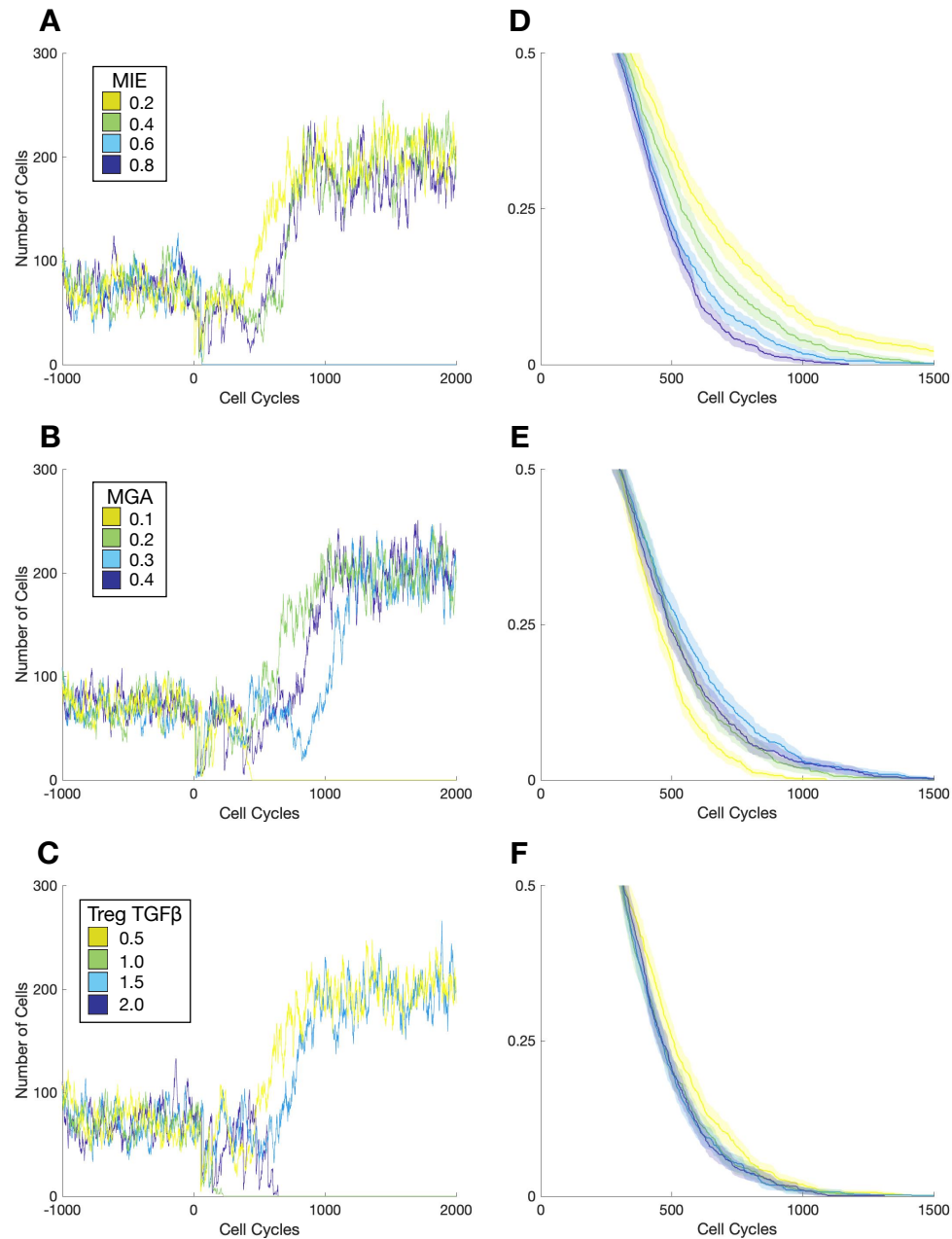


Figure 3: Effects of mesenchymal tumor cell properties on the time to invasion. Trajectories of one patient per cohort including warmup and 2000 cell cycles for **A.** mesenchymal immune evasion (MIE); **B.** mesenchymal growth arrest (MGA); **C.** Production of TGF- β by Tregs. **D.** Survival curve corresponding to changes in the parameter MIE (A) for a patient cohort of 1000. Shaded region represents the 95% confidence interval over the cohort. **E.** Survival curve corresponding to changes in MGA. **F.** Survival curve corresponding to changes in Treg production of TGF- β .

255 of each, alongside the effects of TGF- β through its production by Tregs. As MIE increases, the
256 invasion-free survival decreases (Fig. 3A) for all sets of parameters studied: as the subpopulation
257 of invasive cells becomes more resistant to immune clearance, the tumor as a whole grows more
258 resilient and thus can grow faster (Fig. 3D).

259 The relationship between MGA and invasion-free survival times displays a very different
260 trend, and is non-monotonic with a local maximum appearing. For small values of MGA,
261 increasing the MGA parameter results in increasing the invasion-free survival (Fig 3B, E).
262 However for large values of MGA, invasion-free survival times decrease. This is explored further
263 below.

264 TGF- β varies according to its production by tumor cells and its production by Tregs. Here
265 we assess the effects of varying the production of TGF- β by Tregs on invasion-free survival (Fig
266 3C, F). We find that at lower production rates of TGF- β , the survival curve initially declines
267 faster whereas higher production rates result in a steeper drop off in survival later. This is
268 due to the possibility that the immune system rapidly clears the tumor upon influx of adaptive
269 immune cells. A higher production of TGF- β by the Tregs mitigates this possibility.

270 **3.4 A key EMT regime maximizes cancer-free survival time under chronic in-** 271 **flammation**

272 To investigate how competing interactions within the inflammatory tumor microenvironment
273 affect EMT, we explored the effects of varying inflammation on invasion-free survival. Patient
274 cohorts were simulated under different inflammation regimes: permanently low inflammation;
275 permanently high inflammation; or variable (periodic high/low) inflammation. Compared to
276 the other inflammation states, permanently high inflammation results in outcomes that vary
277 more subtly with changes in the mesenchymal parameters (Fig. 4). When the inflammation
278 state is either permanently or temporarily low, surprising trends emerge. In both these cases,
279 invasion-free survival time is negatively correlated with MIE, and a local maximum for the
280 invasion-free survival time is found with respect to MGA (close to $\Delta_{MGA} = 0.2$).

281 These differences in the mean invasion-free survival lead to striking variation in outcomes:
282 tumors can be contained *in situ* for up to twice as long as they would otherwise be simply
283 by varying the rates of mesenchymal growth arrest. These predictions point to intriguing
284 therapeutic outcomes: a patient suffering intermittent high inflammatory attacks will benefit
285 directly from EMT-directed therapies, however patients for whom a relatively high inflammation
286 state is observed continuously will not obtain this benefit.

287 When MIE is varied under different inflammation cycling schemes, for all the periodic
288 inflammation schemes studied, increasing MIE will decrease the invasion-free survival (i.e.
289 worsen cancer progression and prognosis) (Fig. 4B). In the case of continuously high inflamma-
290 tion, the effects of MIE are minimal. Thus, under any inflammation regime with periods of low
291 inflammation, as we might intuitively assume, any reduction in mesenchymal immune evasion
292 will lead to improvements in patient outcomes.

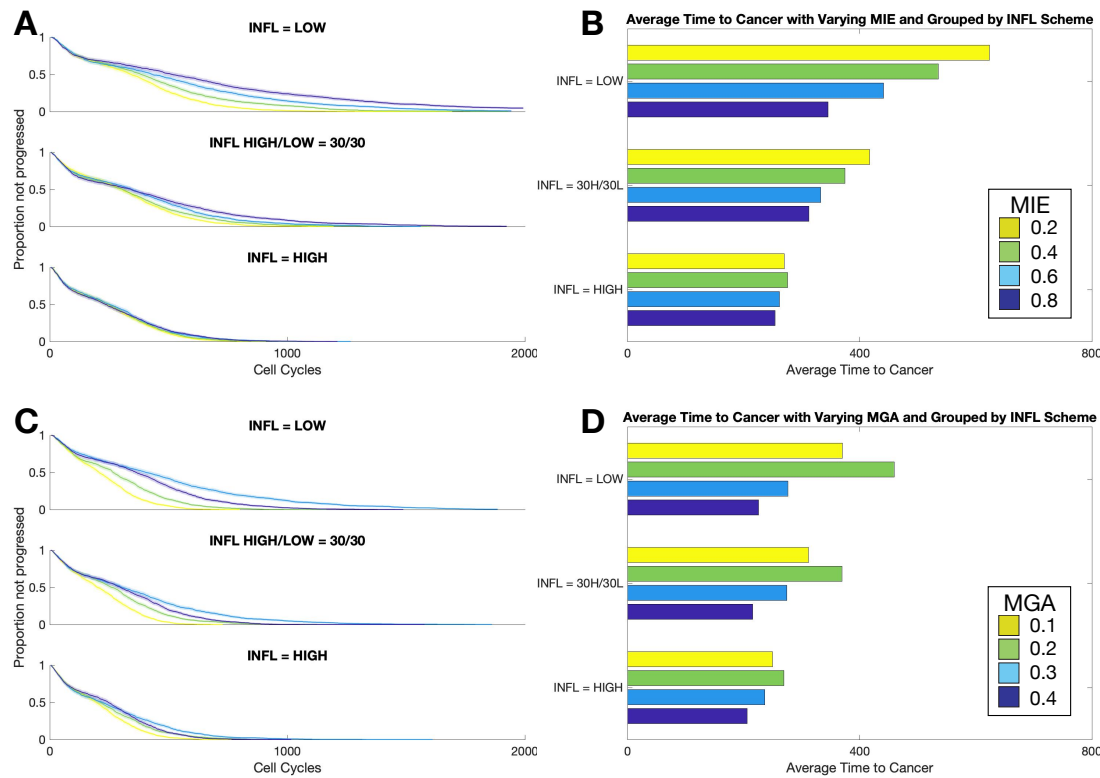


Figure 4: Effects of inflammation on the time to invasion under different cycling schemes. **A-B.** As MIE varies, survival curves (each of 200 patients) and corresponding bar plots to summarize the mean Time to Cancer for each cohort are shown. **C-D.** As MGA varies, survival curves and corresponding bar plots to summarize the mean Time to Cancer for each cohort are shown.

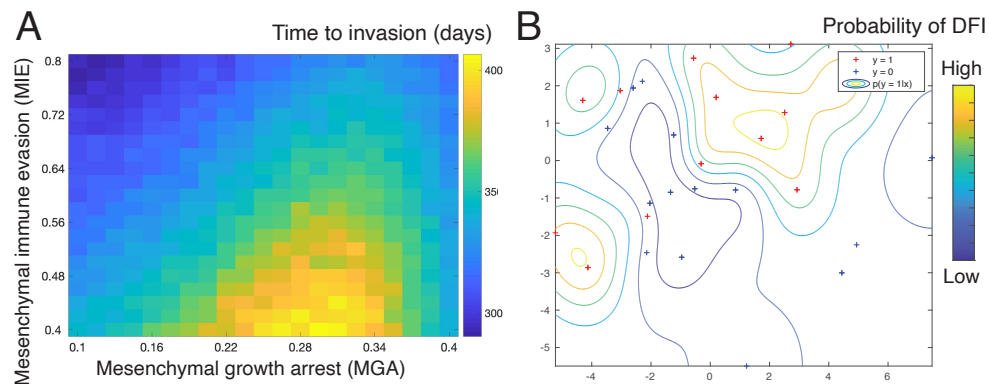


Figure 5: **A.** Summary of the effects of MIE and MGA on invasion-free survival. **B.** Bayesian classification model applied to liver hepatocellular carcinoma (LIHC). Patients projected into 2D by principle components analysis to determine most probable regions of disease-free interval (DFI). Two local maxima are identified, separated by XXXX.

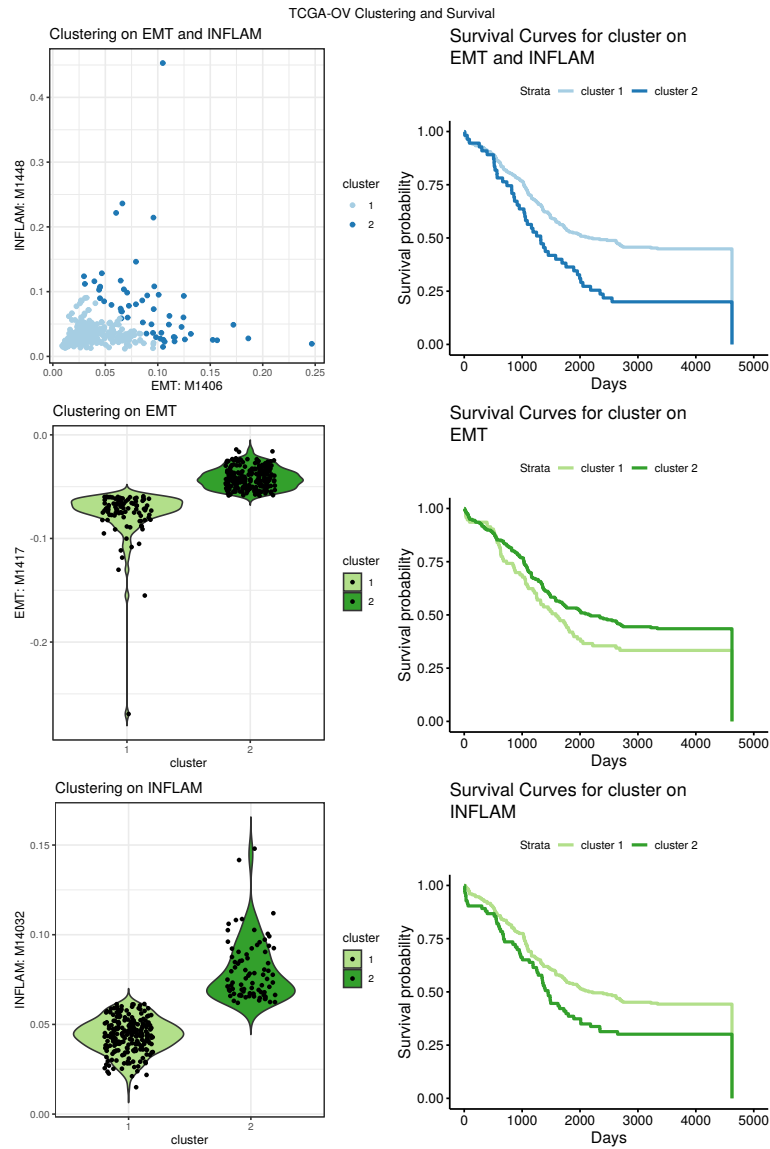


Figure 6: A. K-means clustering of OV using gene ontology terms indicative of EMT and inflammation signatures ($k = 2$). B. Survival plots corresponding to the clustering on EMT and inflammation. C. K-means clustering of OV using gene ontology terms indicative of an EMT signature ($k = 2$). D. Survival plots corresponding to the clustering on EMT. E. K-means clustering of OV using gene ontology terms indicative of inflammation ($k = 2$). F. Survival plots corresponding to the clustering on inflammation.

293 **3.5 Analysis of data from TCGA supports model predictions: EMT phenotypic
294 properties worsen patient outcomes**

295 To compare these model predictions with experimental studies, we analyzed data from The
296 Cancer Genome Atlas (TCGA) [51]. We studied the effects of immune interactions and EMT on
297 cancer prognosis, especially on tumors for which inflammation is known to play an important
298 role, such as those of the colon, or pancreas, or liver [52, 53]. The TCGA Pan-Cancer Clinical
299 Data Resource provides multiple computed clinical endpoints for pancreatic cancer (PAAD) [54].
300 Here, we focus on the disease-free interval (DFI) and the overall survival (OS). A tumor with a
301 short DFI will likely undergo rapid progression post-treatment. We thus expect the distance
302 between DFI and OS to be small for a rapidly progressing tumor, following initial detection. We
303 can therefore characterize tumors as either rapidly progressing or slowly progressing by defining
304 a threshold for the ratio DFI/OS. We selected tumors for which Clinical Data Resource profiles
305 indicated slow progression (ovarian, OV; skin cutaneous melanoma, SKCM; liver hepatocellular
306 carcinoma, LIHC) and two tumors whose profiles indicated rapid progression (pancreatic cancer,
307 PAAD; lung adenocarcinoma, LUAD).

308 The effects on cancer progression of mesenchymal phenotypic properties predicted by the
309 model are summarized in Fig. 5A. Where, for a given value of MIE, there is an optimal value of
310 MGA that maximizes invasion-free survival. We use two models to compare these predictions
311 with TCGA data: a Bayesian supervised classification model, and survival analysis with k-means
312 clustering (see Methods). The classification model applied to liver carcinoma identifies local
313 maxima that promote survival, demonstrating intriguing similarities with model results (Fig.
314 5B). **Classification plots for OV/PAAD in SI**

315 For each cohort of patients for which we have clinical and expression data, we cluster
316 the patients via k-means ($n = 2$) against gene ontologies relating to either: EMT signature
317 alone, inflammatory signature alone, or the combination of both signatures. We then plot the
318 corresponding survival curves (using the OS from TCGA) for each of the two groups (Fig. 6
319 for ovarian cancer and Fig. 7 for pancreatic cancer). We see that for both these tumor types,
320 survival is affected by the gene ontology signature, and the combination of both EMT and
321 inflammatory signatures has a greater impact on survival than the effects of either EMT or
322 inflammation alone. This suggests that in considering interactions between cancer and the
323 immune system, it is of critical importance to consider the effects of EMT, as these can significant
324 impact outcomes and should not be overlooked.

325 The model considered here studies tumor progression from *in situ* to invasive disease from
326 a homogeneous initial point, whereas the data address how cancer may progress following
327 treatment, thus comparisons between model and data should be made carefully. Nonetheless
328 the core cellular tumor dynamics are at play both during the tumor progression addressed by
329 the model, and post-treatment progression described in data from TCGA. Of particular note,
330 the plasticity of tumor cells allows them to evade treatment by undergoing post-treatment
331 processes resembling the de-novo appearance of cancer [55].

332 **4 Discussion**

333 Despite the intense research focus on interactions between cancer and the immune system, and
334 well as on the effects of EMT on cancer, there has not previously, to the best of our knowledge,

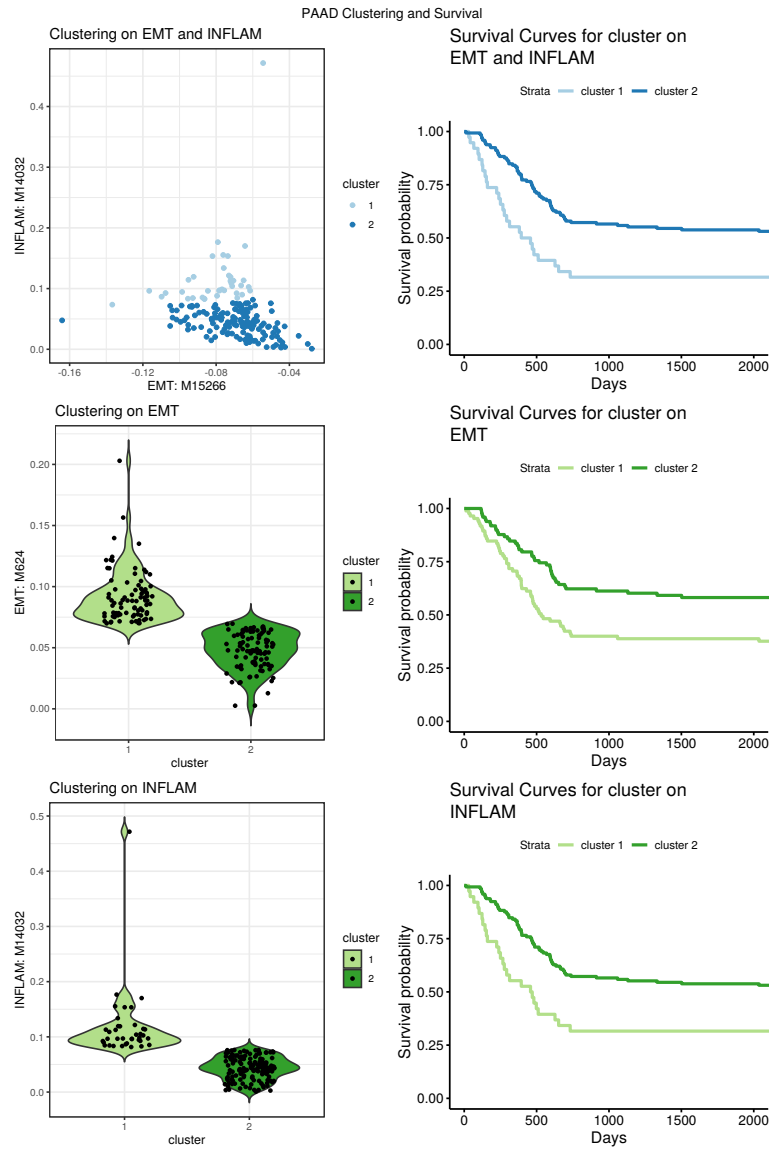


Figure 7: A. K-means clustering of PAAD using gene ontology terms indicative of EMT and inflammation signatures ($k = 2$). B. Survival plots corresponding to the clustering on EMT and inflammation. C. K-means clustering of PAAD using gene ontology terms indicative of an EMT signature ($k = 2$). D. Survival plots corresponding to the clustering on EMT. E. K-means clustering of PAAD using gene ontology terms indicative of inflammation ($k = 2$). F. Survival plots corresponding to the clustering on inflammation.

been a model developed that combines these three components. Here we studied cancer, the immune system, and EMT, during the progression from an *in situ* tumor to invasive disease. We saw this as a particularly pressing need given the shared factors influencing all these components, such as TGF- β . We used an individual cell-based model framework to describe the multiscale processes that can lead to cancer: DNA damage occurs during the cell cycle and this can lead to mutations in pathways that affect cell fitness, which in turn affects the cell population dynamics. Population dynamics are also influenced by the intrinsic state of the cell (through EMT), and extrinsic immune factors.

We found that this model recapitulated invasion-free survival dynamics. Using global parameter sensitivity analysis, we identified parameters exerting key control over model behavior. Focusing on these led us to identify that increasing mesenchymal immune evasion and increasing Treg TGF- β production both lead to shorter invasion-free survival times. However, varying the level of inflammation led to paradoxical effects with regards to mesenchymal growth arrest: under regimes with periods of low inflammation, an optimal level of mesenchymal growth arrest can improve outcomes and maximize the invasion-free survival. To test these predictions, we performed unsupervised analysis of pancreatic cancer data from The Cancer Genome Atlas, and looked at survival across groups with *rapidly progressing* or *slowly progressing* tumors. We found that combinatorial effects of EMT + inflammation increased the differences in survival between groups.

To capture the essential characteristics of the model, we summarized *in silico* patient studies with a single parameter: the invasion-free survival time (see Fig. 1B for a reminder of the full model heterogeneity). There are, of course, many trajectories that result in cancer progression. Analysis of the transient cell dynamics in cancer *in situ* and during progression is a pressing need to shed insight into cellular biomarkers of cancer.

The predictions of this model offer promising leads in elucidating the competing roles of immune cells and EMT during tumor progression, but much remains to be done. Further development of the inflammation module of this model is important given the large and sometimes paradoxical roles that the inflammatory state exerts on tumor cells and invasion-free survival (Figs. 2 and 4B, D). Currently, inflammation is modeled as independently cycling between high and low schemes, however several model components contribute to the inflammatory state. This can be modeled for example by assuming that the level of inflammation depends on the number of and the degree of mutations that tumor cells harbor. The competing roles that TGF- β play throughout the tumor and its microenvironment also warrant further investigation. We found that – below a certain threshold – reduction of TGF- β increases the time to invasion (Fig. 3E): reducing TGF- β in the TME can benefit survival. Recent experiment work in support of this demonstrated that TGF- β drives tumor suppression in pancreatic cancer by promoting EMT [56]. TGF- β , however, is implicated in numerous other cellular signaling processes, and changing TGF- β concentration even in a local environment could have large off-target effects. Indeed, it has been shown that TGF- β promotes invasion and heterogeneity while suppressing cell proliferation in squamous cell carcinoma [57]. To help account for such complex circuitry, future work should incorporate the effects of signaling factors downstream of TGF- β on tumor cell dynamics. We are currently developing a larger TGF- β signaling pathway component within the full model that permits crosstalks between ETCs, MTCs, and immune cell populations through transcriptional signaling activity.

Further *in silico* work on this model and its extensions will explore (and exploit) the

380 heterogeneity of tumor evolution in greater depth. Tumor heterogeneity greatly enhances the
381 capabilities of the tumor to evade immune effects. Studying the consequences of this increased
382 heterogeneity following disease incidence, i.e. decanalization [58], is too-often sidelined,
383 despite mounting evidence in support of its prominent role in cancer evolution [59–61]. Despite
384 these challenges (for which disease complexity is often in part responsible), great progress
385 has been and continues to be made. As we are rapidly approaching a new generation of
386 immunotherapies, it is these very complexities that we must better understand in order to
387 control or eradicate the disease.

388 Acknowledgements

389 Q.N. would like to acknowledge partial support for this work from National Institutes of Health
390 grants R01GM123731, U01AR073159, and U54-CA217378; National Science Foundation grants
391 DMS1562176 and DMS1763272; Simons Foundation grant (594598); and the Jayne Koskinas
392 Ted Giovanis Foundation for Health and Policy joint with the Breast Cancer Research Foundation.
393 A.L.M. would like to acknowledge partial support for this work from an American Cancer Society
394 grant #IRG-16-181-57.

395 References

- 396 [1] Dillekås H, Rogers MS, Straume O. Are 90% of deaths from cancer caused by metastases? Cancer Medicine. 2019;;
- 397 [2] Ryan BM, Faupel-Badger JM. The hallmarks of premalignant conditions: a molecular basis for cancer prevention. In: Seminars in oncology. vol. 43. Elsevier; 2016. p. 22–35.
- 400 [3] De Visser KE, Eichten A, Coussens LM. Paradoxical roles of the immune system during cancer development. Nature Reviews Cancer. 2006;6(1):24.
- 402 [4] Finn OJ. Immuno-oncology: understanding the function and dysfunction of the immune system in cancer. Annals of Oncology. 2012;23(Suppl 8):vii6–viii9. doi:10.1093/annonc/mds256.
- 405 [5] Ruffell B, DeNardo DG, Affara NI, Coussens LM. Lymphocytes in cancer development: polarization towards pro-tumor immunity. Cytokine & Growth Factor Reviews. 2010;21(1):3–10.
- 408 [6] Hu B, Elinav E, Huber S, Booth CJ, Strowig T, Jin C, et al. Inflammation-induced tumorigenesis in the colon is regulated by caspase-1 and NLRC4. Proceedings of the National Academy of Sciences. 2010;107(50):21635–21640. doi:10.1073/pnas.1016814108.
- 411 [7] Balkwill F, Mantovani A. Inflammation and cancer: back to Virchow? The Lancet. 2001;357(9255):539–545. doi:10.1016/S0140-6736(00)04046-0.
- 413 [8] Guo Y, Nie Q, MacLean AL, Li Y, Lei J, Li S. Multiscale Modeling of Inflammation-Induced Tumorigenesis Reveals Competing Oncogenic and Oncoprotective Roles for Inflammation. Cancer Research. 2017;77(22):6429–6441. doi:10.1158/0008-5472.CAN-17-1662.

- 416 [9] Pardoll DM. The blockade of immune checkpoints in cancer immunotherapy. *Nature*
417 *Reviews Cancer*. 2012;12(4):252.
- 418 [10] Restifo NP, Dudley ME, Rosenberg SA. Adoptive immunotherapy for cancer: harnessing
419 the T cell response. *Nature Reviews Immunology*. 2012;12(4):269.
- 420 [11] Ying Z, Huang XF, Xiang X, Liu Y, Kang X, Song Y, et al. A safe and potent anti-CD19 CAR
421 T cell therapy. *Nature medicine*. 2019; p. 1.
- 422 [12] Schreiber RD, Old LJ, Smyth MJ. Cancer Immunoediting: Integrating Immunity's
423 Roles in Cancer Suppression and Promotion. *Science*. 2011;331(6024):1565–1570.
424 doi:10.1126/science.1203486.
- 425 [13] Nieto MA, Huang RYJ, Jackson RA, Thiery JP. EMT: 2016. *Cell*. 2016;166(1):21–45.
- 426 [14] Nie Q. Stem cells: a window of opportunity in low-dimensional EMT space. *Oncotarget*.
427 2018;9(61). doi:10.18632/oncotarget.25852.
- 428 [15] Sha Y, Haensel D, Gutierrez G, Du H, Dai X, Nie Q. Intermediate cell states in epithelial-
429 to-mesenchymal transition. *Physical Biology*. 2019;16(2):021001. doi:10.1088/1478-
430 3975/aaf928.
- 431 [16] Hong T, Watanabe K, Ta CH, Villarreal-Ponce A, Nie Q, Dai X. An Ovol2-Zeb1 mutual
432 inhibitory circuit governs bidirectional and multi-step transition between epithelial and
433 mesenchymal states. *PLoS Computational Biology*. 2015;11(11):e1004569.
- 434 [17] Jolly MK, Jia D, Boareto M, Mani SA, Pienta KJ, Ben-Jacob E, et al. Coupling the modules of
435 EMT and stemness: A tunable ‘stemness window’ model. *Oncotarget*. 2015;6(28):25161–
436 25174.
- 437 [18] Moris N, Pina C, Martinez Arias A. Transition states and cell fate decisions in epigenetic
438 landscapes. *Nature Reviews Genetics*. 2016;17(11):693–703. doi:10.1038/nrg.2016.98.
- 439 [19] MacLean AL, Hong T, Nie Q. Exploring intermediate cell states through
440 the lens of single cells. *Current Opinion in Systems Biology*. 2018;9:32–41.
441 doi:10.1016/j.coisb.2018.02.009.
- 442 [20] Ta CH, Nie Q, Hong T. Controlling stochasticity in epithelial-mesenchymal transition
443 through multiple intermediate cellular states. *Discrete and Continuous Dynamical Systems*
444 - Series B. 2016;21(7):2275–2291. doi:10.3934/dcdsb.2016047.
- 445 [21] Rackauckas C, Schilling TF, Nie Q. Mean-Independent Noise Control of Cell Fates via
446 Intermediate States. *iScience*. 2018;0(0). doi:10.1016/j.isci.2018.04.002.
- 447 [22] Woods K, Pasam A, Jayachandran A, Andrews MC, Cebon J. Effects of epithelial to
448 mesenchymal transition on T cell targeting of melanoma cells. *Frontiers in Oncology*.
449 2014;4:367.
- 450 [23] Terry S, Savagner P, Ortiz-Cuaran S, Mahjoubi L, Saintigny P, Thiery JP, et al. New insights
451 into the role of EMT in tumor immune escape. *Molecular Oncology*. 2017;11(7):824–846.

- 452 [24] Peinado H, Olmeda D, Cano A. Snail, Zeb and bHLH factors in tumour progression: an
453 alliance against the epithelial phenotype? *Nature Reviews Cancer.* 2007;7:415 EP –.
- 454 [25] Lim J, Thiery JP. Epithelial-mesenchymal transitions: insights from development. *Development.* 2012;139(19):3471–3486.
- 455 [26] Shi C, Chen Y, Chen Y, Yang Y, Bing W, Qi J. CD4+ CD25+ regulatory T cells promote
456 hepatocellular carcinoma invasion via TGF- β 1-induced epithelial–mesenchymal transition.
457 *OncoTargets and therapy.* 2019;12:279.
- 458 [27] Anderson ARA, Chaplain MAJ. Continuous and discrete mathematical models of tumor-
459 induced angiogenesis. *Bulletin of Mathematical Biology.* 1998;60(5):857–899.
- 460 [28] Sherratt Jonathan A , Nowak Martin A . Oncogenes, anti-oncogenes and the immune
461 response to cancer : a mathematical model. *Proceedings of the Royal Society of London*
462 *Series B: Biological Sciences.* 1992;248(1323):261–271. doi:10.1098/rspb.1992.0071.
- 463 [29] Pillis LGd, Radunskaya AE, Wiseman CL. A Validated Mathematical Model of Cell-
464 Mediated Immune Response to Tumor Growth. *Cancer Research.* 2005;65(17):7950–7958.
465 doi:10.1158/0008-5472.CAN-05-0564.
- 466 [30] Kim E, Kim JY, Smith MA, Haura EB, Anderson ARA. Cell signaling heterogeneity
467 is modulated by both cell-intrinsic and -extrinsic mechanisms: An integrated
468 approach to understanding targeted therapy. *PLOS Biology.* 2018;16(3):e2002930.
469 doi:10.1371/journal.pbio.2002930.
- 470 [31] Gallaher J, Babu A, Plevritis S, Anderson ARA. Bridging Population and Tissue Scale
471 Tumor Dynamics: A New Paradigm for Understanding Differences in Tumor Growth and
472 Metastatic Disease. *Cancer Research.* 2014;74(2):426–435. doi:10.1158/0008-5472.CAN-
473 13-0759.
- 474 [32] Gallaher JA, Enriquez-Navas PM, Luddy KA, Gatenby RA, Anderson ARA. Spatial Heterogeneity
475 and Evolutionary Dynamics Modulate Time to Recurrence in Continuous and
476 Adaptive Cancer Therapies. *Cancer Research.* 2018;78(8):2127–2139. doi:10.1158/0008-
477 5472.CAN-17-2649.
- 478 [33] An G, Kulkarni S. An agent-based modeling framework linking inflammation and cancer
479 using evolutionary principles: Description of a generative hierarchy for the hallmarks of
480 cancer and developing a bridge between mechanism and epidemiological data. *Mathematical*
481 *Biosciences.* 2015;260:16–24. doi:10.1016/j.mbs.2014.07.009.
- 482 [34] Serre R, Benzekry S, Padovani L, Meille C, André N, Ciccolini J, et al. Mathematical
483 Modeling of Cancer Immunotherapy and Its Synergy with Radiotherapy. *Cancer Research.*
484 2016;76(17):4931–4940. doi:10.1158/0008-5472.CAN-15-3567.
- 485 [35] Louzoun Y, Xue C, Lesinski GB, Friedman A. A mathematical model for pancreatic
486 cancer growth and treatments. *Journal of Theoretical Biology.* 2014;351:74–82.
487 doi:10.1016/j.jtbi.2014.02.028.

- 489 [36] Briones-Orta MA, Levy L, Madsen CD, Das D, Erker Y, Sahai E, et al. Arkadia regulates tu-
490 mor metastasis by modulation of the TGF- β pathway. *Cancer Research*. 2013;73(6):1800–
491 1810. doi:10.1158/0008-5472.CAN-12-1916.
- 492 [37] Lavi O, Greene JM, Levy D, Gottesman MM. The Role of Cell Density and Intratumoral Hetero-
493 geneity in Multidrug Resistance. *Cancer Research*. 2013;doi:10.1158/0008-5472.CAN-
494 13-1768.
- 495 [38] Greene JM, Levy D, Fung KL, Souza PS, Gottesman MM, Lavi O. Modeling intrinsic
496 heterogeneity and growth of cancer cells. *Journal of Theoretical Biology*. 2015;367:262–
497 277. doi:10.1016/j.jtbi.2014.11.017.
- 498 [39] Greene JM, Levy D, Herrada SP, Gottesman MM, Lavi O. Mathematical Modeling
499 Reveals That Changes to Local Cell Density Dynamically Modulate Baseline Vari-
500 tions in Cell Growth and Drug Response. *Cancer Research*. 2016;76(10):2882–2890.
501 doi:10.1158/0008-5472.CAN-15-3232.
- 502 [40] Cho H, Levy D. Modeling the Dynamics of Heterogeneity of Solid Tumors in Re-
503 sponse to Chemotherapy. *Bulletin of Mathematical Biology*. 2017;79(12):2986–3012.
504 doi:10.1007/s11538-017-0359-1.
- 505 [41] Benzekry S, Lamont C, Barbolosi D, Hlatky L, Hahnfeldt P. Mathematical Modeling of
506 Tumor–Tumor Distant Interactions Supports a Systemic Control of Tumor Growth. *Cancer
507 Research*. 2017;77(18):5183–5193. doi:10.1158/0008-5472.CAN-17-0564.
- 508 [42] Owen MR, Stamper IJ, Muthana M, Richardson GW, Dobson J, Lewis CE, et al. Mathemat-
509 ical Modeling Predicts Synergistic Antitumor Effects of Combining a Macrophage-Based,
510 Hypoxia-Targeted Gene Therapy with Chemotherapy. *Cancer Research*. 2011;71(8):2826–
511 2837. doi:10.1158/0008-5472.CAN-10-2834.
- 512 [43] West J, You L, Brown J, Newton PK, Anderson AR. Towards multi-drug adaptive therapy.
513 bioRxiv. 2018; p. 476507. doi:10.1101/476507.
- 514 [44] de Pillis LG, Radunskaya AE. Modeling tumor–immune dynamics. In: *Mathematical
515 Models of Tumor-Immune System Dynamics*. Springer; 2014. p. 59–108.
- 516 [45] Morris MD. Factorial sampling plans for preliminary computational experiments. *Techno-
517 metrics*. 1991;33(2):161–174.
- 518 [46] Sohier H, Farges JL, Piet-Lahanier H. Improvement of the Representativity of the Morris
519 Method for Air-Launch-to-Orbit Separation. *IFAC Proceedings Volumes*. 2014;47(3):7954–
520 7959.
- 521 [47] Kirk PDW, Thorne T, Stumpf MPH. Model selection in systems and synthetic biology. *Cur-
522 rent Opinion in Biotechnology*. 2013;24(4):767–774. doi:10.1016/j.copbio.2013.03.012.
- 523 [48] Gallaher J, Hawkins-Daarud A, Massey SC, Swanson K, Anderson ARA. Hybrid approach
524 for parameter estimation in agent-based models. *bioRxiv*. 2017;doi:10.1101/175661.

- 525 [49] Warne D, Baker RE, Simpson MJ. Simulation and inference algorithms for stochastic
526 biochemical reaction networks: from basic concepts to state-of-the-art. *Journal of The
527 Royal Society Interface*. 2019;16(151):20180943. doi:10.1098/rsif.2018.0943.
- 528 [50] Lambert B, MacLean AL, Fletcher AG, Combes AN, Little MH, Byrne HM. Bayesian
529 inference of agent-based models: a tool for studying kidney branching morphogenesis.
530 *Journal of Mathematical Biology*. 2018;10(12):106. doi:10.1007/s00285-018-1208-z.
- 531 [51] Weinstein JN, Collisson EA, Mills GB, Shaw KRM, Ozenberger BA, Ellrott K, et al. The
532 cancer genome atlas pan-cancer analysis project. *Nature genetics*. 2013;45(10):1113.
- 533 [52] Greten FR, Grivennikov SI. Inflammation and Cancer: Triggers, Mechanisms, and Conse-
534 quences. *Immunity*. 2019;51(1):27–41.
- 535 [53] Hu B, Elinav E, Huber S, Booth CJ, Strowig T, Jin C, et al. Inflammation-induced tumori-
536 genesis in the colon is regulated by caspase-1 and NLRC4. *Proceedings of the National
537 Academy of Sciences*. 2010;107(50):21635–21640.
- 538 [54] Liu J, Lichtenberg T, Hoadley KA, Poisson LM, Lazar AJ, Cherniack AD, et al. An integrated
539 TCGA pan-cancer clinical data resource to drive high-quality survival outcome analytics.
540 *Cell*. 2018;173(2):400–416.
- 541 [55] Sánchez-Danés A, Larsimont JC, Liagre M, Muñoz-Couselo E, Lapouge G, Brisebarre A,
542 et al. A slow-cycling LGR5 tumour population mediates basal cell carcinoma relapse after
543 therapy. *Nature*. 2018;562(7727):434.
- 544 [56] David C, Huang YH, Chen M, Su J, Zou Y, Bardeesy N, et al. TGF- β Tumor Suppression
545 through a Lethal EMT. *Cell*. 2016;164(5):1015–1030. doi:10.1016/j.cell.2016.01.009.
- 546 [57] Oshimori N, Oristian D, Fuchs E. TGF- β Promotes Heterogeneity and Drug Resistance in
547 Squamous Cell Carcinoma. *Cell*. 2015;160(5):963–976. doi:10.1016/j.cell.2015.01.043.
- 548 [58] Gibson G. Decanalization and the origin of complex disease. *Nature Reviews Genetics*.
549 2009;10(2):134–140. doi:10.1038/nrg2502.
- 550 [59] Cyll K, Ersvær E, Vlatkovic L, Pradhan M, Kildal W, Kjær MA, et al. Tumour heterogeneity
551 poses a significant challenge to cancer biomarker research. *British Journal of Cancer*.
552 2017;117(3):367–375. doi:10.1038/bjc.2017.171.
- 553 [60] Punt CJA, Koopman M, Vermeulen L. From tumour heterogeneity to advances in precision
554 treatment of colorectal cancer. *Nature Reviews Clinical Oncology*. 2017;14(4):235–246.
555 doi:10.1038/nrclinonc.2016.171.
- 556 [61] Dagogo-Jack I, Shaw AT. Tumour heterogeneity and resistance to cancer therapies. *Nature
557 Reviews Clinical Oncology*. 2018;15(2):81–94. doi:10.1038/nrclinonc.2017.166.